A distinct subpopulation of CD25^{-} T-follicular regulatory cells localizes in the germinal centers

James Badger Wing[a], Yohko Kitagawa[a], Michela Locci[b], Hannah Hume[a], Christopher Tay[a], Takayoshi Morita[a], Yujiro Kidani[a], Kyoko Matsuda[c], Takeshi Inoue[d], Tomohiro Kurosaki[d,e], Shane Crotty[b], Cevayir Coban[c], Naganari Ohkura[a], and Shimon Sakaguchi[a,f,1]

[a]Laboratory of Experimental Immunology, WPI Immunology Frontier Research Center (IFReC), Osaka University, Suita 565-0871, Japan; [b]Division of Vaccine Discovery, La Jolla Institute for Allergy and Immunology, La Jolla, CA 92037; [c]Malaria Immunology, IFReC, Osaka University, Suita 565-0871, Japan; [d]Lymphocyte Differentiation, IFReC, Osaka University, Suita 565-0871, Japan; [e]Laboratory of Lymphocyte Differentiation, RIKEN Center for Integrative Medical Sciences, Yokohama, Kanagawa 230-0045, Japan; and [f]Department of Experimental Pathology, Institute for Frontier Medical Sciences, Kyoto University, Kyoto 606-8507, Japan

Contributed by Shimon Sakaguchi, June 7, 2017 (sent for review April 11, 2017; reviewed by Luis Graca and Shohei Hori)

T-follicular helper (Tfh) cells differentiate through a multistep process, culminating in germinal center (GC) localized GC-Tfh cells that provide support to GC-B cells. T-follicular regulatory (Tfr) cells have critical roles in the control of Tfh cells and GC formation. Although Tfh-cell differentiation is inhibited by IL-2, regulatory T (Treg) cell differentiation and survival depend on it. Here, we describe a CD25^{-} subpopulation within both murine and human PD1^{+}CXCR5^{+}Foxp3^{+} Tfr cells. It is preferentially located in the GC and can be clearly differentiated from CD25^{+} non–GC-Tfr, Tfh, and effector Treg (eTreg) cells by the expression of a wide range of molecules. In comparison to CD25^{+} Tfr and eTreg cells, CD25^{-} Tfr cells partially down-regulate IL-2–dependent canonical Treg features, but retain suppressive function, while simultaneously up-regulating genes associated with Tfh and GC-Tfh cells. We suggest that, similar to Tfh cells, Tfr cells follow a differentiation pathway generating a mature GC-localized subpopulation, CD25^{-} Tfr cells.

Treg cell | T-follicular regulatory cell | Tfr cell | germinal center | Tfh cell

T-follicular helper (Tfh) cells have a critical role in the formation and maintenance of germinal center (GC) reactions responsible for the production of high-quality antibodies (1). Tfh cells differentiate in a multistage process beginning with contact with dendritic cells, which provide them with IL-6 and ICOS-ligand, allowing their up-regulation of the lineage-defining transcription factor BCL6 (2–4). This process leads to down-regulation of chemotactic receptors (CCR7 and PSGL1) responsible for maintaining the cells in the T-cell zone and up-regulation of CXCR5, which recognizes CXCL13, enabling the cells to travel to the T/B border. Once the pre-Tfh cells contact cognate B cells and receive further stimulation, they fix the Tfh gene program that allows some Tfh cells to enter the GC and become BCL6^{hi}PD1^{hi}CXCR5^{hi} IL-4 and IL-21, producing GC-Tfh cells (1).

Foxp3-expressing regulatory T (Treg) cells are vital for the maintenance of immune tolerance and homeostasis (5). Loss of Foxp3 expression, in mice or humans, or depletion of total Treg cells leads to spontaneous expansion of GCs and Tfh cells, resulting in the production of autoantibodies and hyperproduction of IgE (6). Treg cells are able to become T-follicular regulatory (Tfr) cells by coopting the Tfh transcriptional program, including the expression of BCL6. This program allows them to access the follicles and GCs, and to provide in situ suppression of antibody production (7–10). However, it is not clear if there is a highly differentiated subset of Tfr cells, equivalent to GC-Tfh cells, in GCs.

We initially identified Treg cells by their high-level expression of the α-chain of the IL-2 receptor (CD25) (11). IL-2 is important for both the thymic production of Treg cells and their peripheral maintenance because IL-2 signaling via CD25 and STAT5 is essential for Treg proliferation and survival (12). Further, the differentiation of highly activated CD103^{+}KLRG1^{+} effector Treg (eTreg) cells is dependent on the expression of BLIMP-1 (13). Conversely, Tfh cells are CD25^{lo} and BCL6 is known to be a reciprocal regulator of BLIMP-1 (2). As a result, Tfh cells are directly inhibited by IL-2/STAT5–driven induction of BLIMP-1 expression (14, 15). In addition, Tfr cells themselves have been described to express BLIMP-1, but its deletion causes their expansion, suggesting that BLIMP-1 acts to inhibit their formation (10), whereas loss of BCL6 results in increased expression of BLIMP-1 by Treg cells (7). This finding raises the question of how Tfr cells are able to balance these seemingly contradictory signals. Here, we describe that Tfr cells can be subdivided into CD25^{+} and CD25^{-} subpopulations and that the CD25^{-} Tfr cells lose part of their IL-2–dependent Treg identity in exchange for enhanced expression of BCL6 and other Tfh-related genes, which, in turn, allows them to travel to the GC. As such, we identify CD25^{-}CXCR5^{hi} PD1^{hi} Treg cells as an IL-2–independent subpopulation of eTreg cells present in both mice and humans.

Results

Identification of CD25^{-} Tfr Cells. To identify Tfr cells in the lymph nodes (LNs) of vaccinated mice, we used a gating structure beginning with CD3^{+}CD4^{+}B220^{-}CD11c^{-}CD11b^{-} live cells before

Significance

T-follicular regulatory (Tfr) cells, a subset of Foxp3-expressing regulatory T (Treg) cells, have a critical role in the control of antibody responses. Whereas Treg cells express CD25 and are dependent on IL-2, Tfr cells also express the transcription factor BCL6 that is inhibited by IL-2 in T-follicular helper (Tfh) cells. In this report, we find that mature Tfr cells in the germinal centers or circulating in human blood down-regulate CD25 and gain a transcriptional signature mixed between Tfh cells and Treg cells while retaining their regulatory function. These cells represent an IL-2–independent branch of effector Treg cells losing CD25 expression but gaining increased expression of Tfh-related markers, such as BCL6 and CXCR5, in both mice and humans.

Author contributions: J.B.W., C.C., and N.O. designed research; J.B.W., Y. Kitagawa, M.L., H.H., C.T., T.M., Y. Kidani, and K.M. performed research; T.I. and T.K. contributed new reagents/analytic tools; J.B.W., Y. Kitagawa, M.L., C.C., and N.O. analyzed data; and J.B.W., Y. Kitagawa, M.L., C.T., S.C., C.C., N.O., and S.S. wrote the paper.

Reviewers: L.G., Faculdade de Medicina da Universidade de Lisboa; and S.H., University of Tokyo.

Conflict of interest statement: S.H. and S.S. have independently collaborated with the same laboratory and have therefore appeared as coauthors in a paper published as Garg G, et al. (2017) Unique properties of thymic antigen-presenting cells promote epigenetic imprinting of alloantigen-specific regulatory T cells. *Oncotarget* 8:35542–35557, although S.S. did so independently and without knowledge of the other's participation in the work, S.H. and S.S. contributed independently to an article regarding nomenclature published as Abbas AK, et al. (2013) Regulatory T cells: Recommendations to simplify the nomenclature. *Nat Immunol* 14:307–308.

Data deposition: All RNA-sequencing datasets have been deposited in DNA Data Bank of Japan, www.ddbj.nig.ac.jp [accession nos. DRA004824 (murine samples) and DRA005364 (human samples)].

[1]To whom correspondence should be addressed. Email: shimon@ifrec.osaka-u.ac.jp.

This article contains supporting information online at www.pnas.org/lookup/suppl/doi:10.1073/pnas.1705551114/-/DCSupplemental.

gating on Foxp3 to discriminate between Treg and non-Treg cells, and then between $CD44^+CD62L^-$ effector/memory T cells and $CD44^-CD62L^+$ naive T cells in each population. As expected, following vaccination, Tfr cells constituted a significant proportion of activated $CD44^+CD62L^-$ Treg cells but were absent in $CD44^-CD62L^+$ naive Treg (nTreg) cells. The $CD44^+CD62L^-$ Treg cells were then further divided into $CXCR5^-$ eTreg cells and $CXCR5^+PD1^+$ Treg cells. CXCR5 staining was confirmed to be specific by the use of a fluorescence minus one control. We found that $CXCR5^+PD1^+$ Treg cells had a bimodal staining pattern of CD25 in both our own data and other published data (10) (Fig. 1*A*), allowing us to identify $CD25^-$ Tfr and $CD25^+$ Tfr cells. The proportion of $CD25^-$ Tfr cells varied by lymphoid organ, with 24 ± 1% in the draining LNs, 57 ± 2% in the spleen, and 73 ± 4% in the Peyer's patches 7 d after vaccination (mean ± SEM; Fig. S1*A*). Naive and effector conventional T (nTconv and eTconv, respectively) cells were defined as $Foxp3^-CXCR5^-CD44^{lo}CD62L^{hi}$ and $Foxp3^-CXCR5^-CD44^{lo}CD62L^{hi}$. Vaccination was required to induce substantial fractions of $CD25^-$ Tfr cells in the spleen and LNs, whereas the Peyer's patches had a constant population of these cells unaffected by vaccination. To supplement this manual gating, we also used Automatic Classification of Cellular Expression by Nonlinear Stochastic Embedding (ACCENSE), a tool that uses a dimensionality reduction technique, t-distributed stochastic neighbor embedding, which allows the visualization of multiple parameters in two dimensions and is useful in the identification of novel subpopulations (16). Here, we took total CD4 T cells from the Peyer's patches and mapped them by expression of PD1, BCL6, CXCR5, Foxp3, and CD25. Treg cells could be seen to form two distinct "islands," one $CD25^-$ and the other $CD25^+$. $PD1^{hi}CXCR5^{hi}BCL6^{hi}$ Treg cells could be seen to be clustering primarily on the $CD25^-$ island, confirming the identification of these cells as a distinct population (Fig. S1*B*).

Because the border between Tfr and non-Tfr cells was indistinct, we also used an approach of sectioning $CD44^+CD62L^-$ Treg cells into populations with increasing levels of CXCR5 and PD1 expression. The percentage of $CD25^-$ Treg cells increased with the level of CXCR5 and PD1 expression to the extent that $CXCR5^{hi}PD1^{hi}$ Treg cells were almost all $CD25^-$ (Fig. 1*B*). We then carried out time course experiments to investigate the formation of these cells. We found that the ratio of Tfh cells among $CD4^+$ T cells peaked at day 7 before resolving, but that $CD25^+$ Tfr cells and GCs peaked at day 14 before resolving (Fig. 1*C*). The highest percentage of $CD25^-$ Tfr cells coincided with the peak of GC formation at day 14. A similar pattern was seen when data were represented as cells per 100,000 lymphocytes (Fig. S1*C*).

The transcription factor BCL6 is essential for the formation of Tfh and Tfr cells (2–4, 7, 10). To confirm the identity of $CD25^-$ Tfr cells, we examined $BCL6^{flox/flox}$ CD4cre mice (BCL6 CD4 cKO). $CD25^-$ Tfr cells, visualized as a $CXCR5^{hi}$ and $CD25^-$ subpopulation within $CD44^+CD62L^-$ Treg cells, were completely abolished in BCL6 CD4 cKO mice, as were Tfr cells (Fig. 1*D*), Tfh cells, and GCs.

$CD25^-$ Tfr Cells Are an Atypical Subpopulation of $CD25^-CD103^-KLRG1^-BLIMP1^{lo}BCL6^{hi}$ eTreg Cells. We then carried out a fuller assessment of the expression of a wide range of Treg and Tfh markers by flow cytometry. In comparison to $CD25^+$ Tfr cells, $CD25^-$ Tfr cells had higher expression of Tfh-related molecules, such as CXCR5, BCL6, PD1, and BTLA (Fig. 2*A* and Fig. S2), and lower CCR7 and PGSL1, although both lacked IL-21 expression. ICOS and TIGIT were more highly expressed by both $CD25^-$ Tfr and $CD25^+$ Tfr cells than either Tfh or Treg cells (Fig. 2*A* and Fig. S2).

In addition to the near-total loss of CD25, $CD25^-$ Tfr cells showed reduced expression of Foxp3, Helios, CD103, KLRG1, GITR, and BLIMP-1 (Fig. 2 *A* and *B* and Fig. S2). However, in

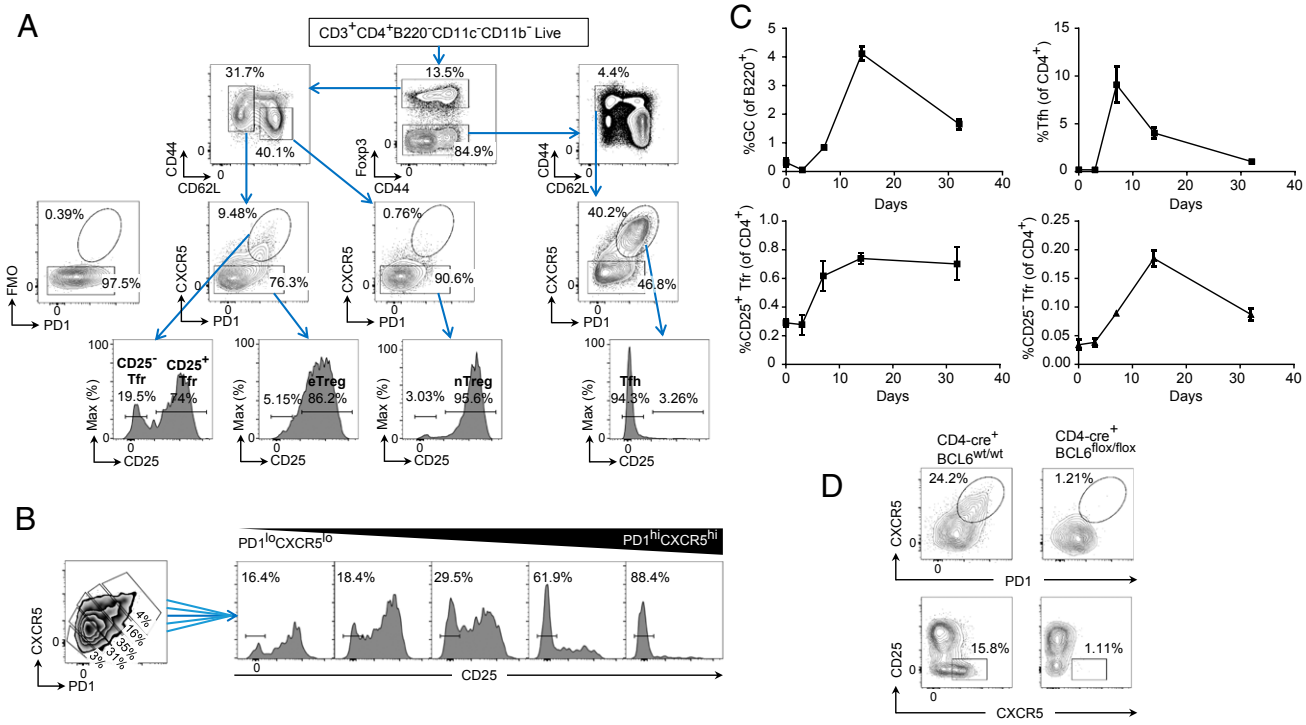

Fig. 1. Identification of $CD25^-$ Tfr cells. Mice were vaccinated s.c. with 100 μg of NP-Ova (Biosearch) in alum, and draining LNs (dLNs) or Peyer's patches were taken at day 7 or the indicated time. (*A*) Gating strategy of $CD25^+$ and $CD25^-$ Tfr cells. Cells were first gated as $CD3^+CD4^+B220^-CD11c^-CD11b^-$Live/Dead-dye$^-$ before the start of the shown gating. The fluorescence minus one (FMO) control is $CD44^+CD62L^-$ Treg cells with anti-CXCR5 omitted. Data are representative of >10 separate experiments. Max, maximum. (*B*) Proportion of $CD25^-$ cells in gated CXCR5 and PD-1 low to high populations in Peyer's patch $CD44^+CD62L^-$ Treg cells. Data are representative of >10 separate experiments. (*C*) Time course of GC, Tfh, $CD25^+$ Tfr, and $CD25^-$ Tfr proportions in dLNs following vaccination at day 0. (*D*) Tfr cells in $BCL6^{flox/flox}$ and $BCL6^{wt/wt}$ CD4-Cre mice, with Peyer's patch T cells pregated on $CD44^+CD62L^-$ Treg cells. (*C* and *D*) Data are pooled from three mice, representative of two separate experiments.

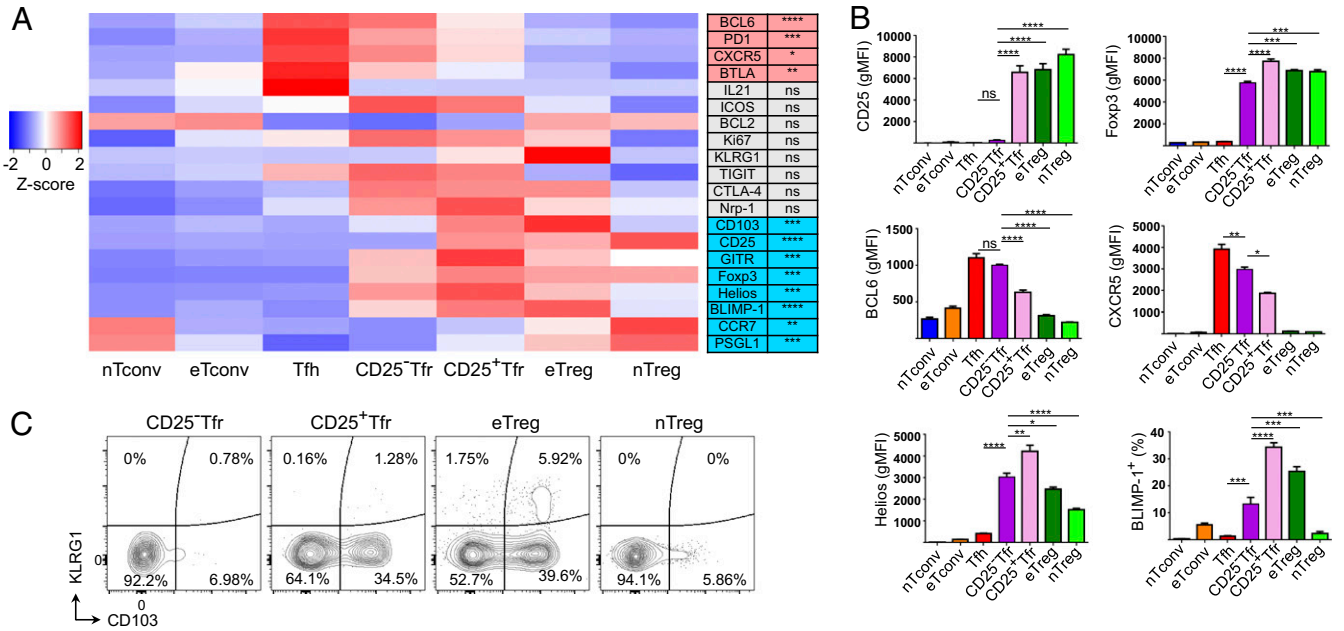

Fig. 2. Protein expression profile of CD25⁻ Tfr cells. Mice were vaccinated s.c. with 100 μg of NP-Ova in alum, and dLNs were taken at day 7 or day 14. (*A*, *Left*) Heat map of geometric mean fluorescence intensity (gMFI; unless indicated otherwise) or percent positive (CD103, Ki-67, IL-21, BLIMP-1, KLRG1) of indicated markers. (*A*, *Right*) Significant differences between CD25⁻ Tfr and CD25⁺ Tfr cells. The scale is the *Z*-score of mean. Data are pooled from three mice, representative of two to four separate experiments. (*B*) Expression of indicated markers by gMFI or percent positive of indicated markers. Mean ± SEM. Data are pooled from three mice, representative of two to four separate experiments. (*C*) Contour plots of KLRG1 and CD103 expression by indicated Treg populations. Data are representative of two separate experiments (*$P \leq 0.05$, **$P \leq 0.01$, ***$P \leq 0.001$, ****$P \leq 0.0001$). ns, not significant.

comparison to nTreg cells, CD25⁻ Tfr cells expressed significantly higher levels of GITR, Helios, Neuropilin-1, BLIMP-1, and CTLA-4, although Foxp3 was still reduced. Additionally, CD25⁻ Tfr cells were clearly separated from Tfh or Tconv cells by expression of a range of Treg-associated markers.

The eTreg cells have been defined as BLIMP-1$^+$KLRG1$^+$CD103$^+$ Treg cells (17). We found that eTreg cells expressed KLRG1 and CD103 and that CD25$^+$ Tfr cells maintained CD103 but had reduced KLRG1 expression, whereas CD25⁻ Tfr cells were double negative, similar to nTreg cells (Fig. 2*C* and Fig. S2). One possible explanation for lower KLRG1, CD103, and BLIMP-1 by CD25⁻ Tfr cells is reduced activation status, even within the CD44$^+$CD62L⁻ gate. We found, however, that CD25⁻ Tfr cells were Ki-67^{hi} and BCL2^{lo} (Fig. 2*A* and Fig. S2), suggesting that they were highly proliferative, apoptosis-prone effector cells and could not be considered at a lower activation status than CD25$^+$ Tfr or eTreg cells.

Tfr Cells Located Within the GCs Express Foxp3 but Not CD25. GC-Tfh cells have been identified as CXCR5^{hi}PD1^{hi} (18), whereas low levels of CCR7 and PGSL-1 also aid their localization to the follicle/GC (19, 20). We hypothesized that because CD25⁻ Tfr cells were CXCR5^{hi}PD1^{hi}CCR7^{lo}PGSL-1^{lo}, they might be preferentially localized in GCs. On examination of spleen sections by confocal microscopy, we found that in the T-cell zone of unvaccinated mouse spleens, the majority of Foxp3-expressing cells also expressed CD25, although this expression was reduced in B-cell follicles (Fig. 3*A*). Following vaccination and formation of GCs, we again observed that most Foxp3$^+$ Treg cells in the T-cell zone expressed CD25, with reduced expression in the follicles and only a small minority of Foxp3$^+$ cells in the GCs expressing CD25 (Fig. 3 *B* and *C*). Similar to our earlier results (Fig. S1*A*), we also found that CD25 expression was lower in the spleen than in the LNs (Fig. 3*C*).

CD25⁻ Tfr Cells Have a Gene Expression Pattern Equidistant Between Tfh and eTreg Cells. To understand the relationship between the gene expression patterns of CD25$^+$ Tfr, CD25⁻ Tfr, Tfh, and eTreg cells more fully, we sorted CD4$^+$B220⁻ cells from vaccinated Foxp3 reporter mice to obtain CD62L⁻CXCR5⁻Foxp3⁻GITR⁻ eTconv, CD62L⁻CXCR5$^+$PD1$^+$Foxp3⁻GITR⁻ Tfh, CD62L⁻CXCR5⁻Foxp3$^+$GITR$^+$CD25$^+$ eTreg, CD62L⁻CXCR5$^+$PD1$^+$GITR$^+$CD25$^+$ CD25$^+$ Tfr, CD62L⁻CXCR5$^+$PD1$^+$Foxp3$^+$GITR$^+$CD25⁻ CD25⁻ Tfr, and CD62L$^+$CXCR5⁻PD1⁻Foxp3$^+$GITR$^+$CD25$^+$ nTreg cells and assessed gene expression of each population by RNA-sequencing (RNA-Seq). To allow the generation of a gene expression signature that was able to differentiate fully between Tfh and Treg cells, we compared Tfh cells with eTreg cells and generated a list of differentially expressed (DE) genes ($P < 0.01$ false discovery rate, ≥ twofold change). This comparison identified 1,046 DE genes (Dataset S1), enabling us to generate heat maps of the top 25 Tfh up-regulated and top 25 Treg up-regulated (Tfh down-regulated) genes from the list. CD25⁻ Tfr cells strongly up-regulated Tfh-related genes (Fig. 4*A*) and partially down-regulated Treg genes (Fig. 4*B*). CD25$^+$ Tfr cells had a similar but weaker expression pattern. A heat map of the full list of DE genes also demonstrated the same pattern (Fig. S3*A*). In addition, analysis of a list of known Tfh genes, such as Sphingosine-1-phosphate receptor 2 (S1PR2), a molecule previously demonstrated to be important for the retention of Tfh in the GC, demonstrated a similar expression pattern (21) (Fig. S3*B*). To confirm this finding, we performed gene set enrichment analysis (GSEA) using the top 250 Tfh up-regulated and Treg up-regulated genes from our previous DE list as the gene set database. CD25⁻ Tfr cells were significantly enriched for Tfh up-regulated genes, whereas CD25$^+$ Tfr cells were significantly enriched for Treg up-regulated genes (Fig. 4*C*). Further analysis also demonstrated that CD25⁻ Tfr cells were significantly enriched for genes previously identified as up-regulated by BCL6^{hi} GC-Tfh cells in comparison to CD4 T cells (22) (Fig. S3*C*).

Analysis of a wide range of Treg suppressive molecules (e.g., CTLA-4, TIGIT, TGF-β1), and other key Treg markers demonstrated that CD25⁻ Tfr cells retained the expression of most known suppressive molecules (Fig. 4*D*). Only *Il10*, *GrzB* (encoding the protein Granzyme B), and *Itgae* (encoding the protein CD103) were DE ($P < 0.01$, ≥ twofold change) between CD25$^+$ Tfr and CD25⁻ Tfr cells.

The visual impression given by the heat maps was then further confirmed by principal component analysis (Fig. 4*E*) and Euclidian distance (Fig. S3*D*), demonstrating that CD25⁻ Tfr cells were

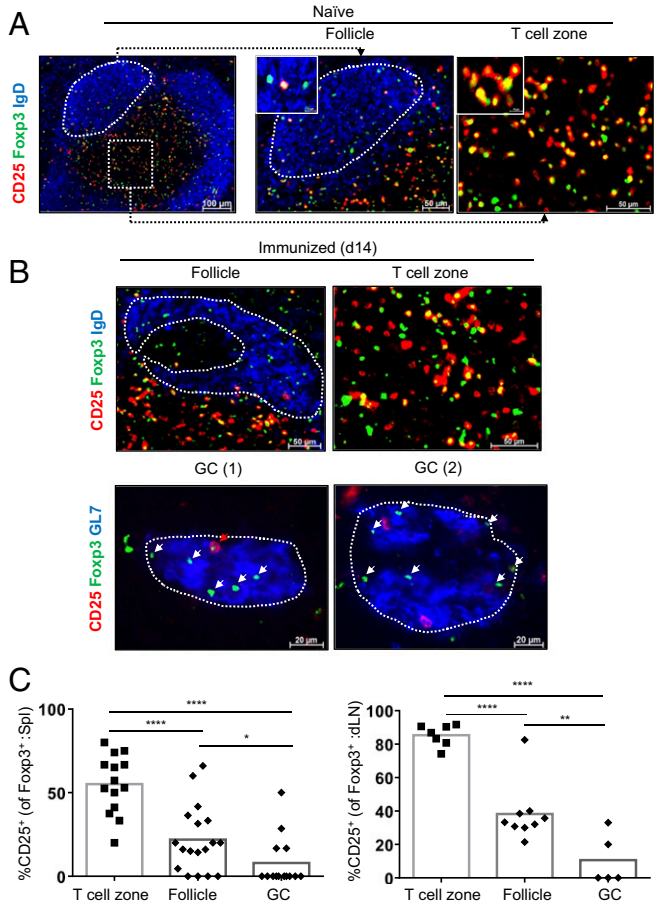

Fig. 3. Localization of CD25$^-$ Tfr cells. Mice were/were not vaccinated s.c. and i.p. with 100 μg of NP-Ova in alum and then killed 14 d later. Spleens and dLNs were taken and fixed in 2% paraformaldehyde. Sections were then stained, and expression of Foxp3, CD25, and IgD or Foxp3, CD25, and GL7 was assessed by immunohistochemistry. (*A*) Foxp3 and CD25 expression by Treg cells in the follicle and T-cell zones from the spleens of unvaccinated mice. (*B*) Foxp3 and CD25 expression of Treg cells in the follicle, T-cell zones, and GC from spleens of vaccinated mice. CD25, Foxp3, and IgD expression (*Upper*) and CD25, Foxp3, and GL7 expression (*Lower*) are shown. White arrows denote Foxp3$^+$CD25$^-$ cells, and the red arrow denotes a Foxp3$^+$ CD25$^+$ cell. (*C*) Proportion of CD25 expression within Foxp3$^+$ cells in the follicle, T-cell zone, and GC from spleens (Spl) (*Left*) and dLNs (*Right*). Each data point represents a separate field. Data are pooled from three mice, representative of two separate experiments (*$P \leq 0.05$, **$P \leq 0.01$, ****$P \leq 0.0001$).

shifted toward Tfh cells, whereas CD25$^+$ Tfr cells were closer to eTreg and nTreg cells. More precisely, we found that the Euclidian distances to the Tfh and eTreg gene expression signatures were almost equidistant for CD25$^-$ Tfr cells, confirming that these cells are equally poised between these fates (Fig. 4*F*). Full lists of differentially up-regulated genes between CD25$^-$ Tfr, CD25$^+$ Tfr, eTreg, and Tfh cells are provided in Dataset S1.

Although we noted the up-regulation of some myeloid-related genes in the Tfr subpopulations, it could be attributed to some contamination due to sorting these rare cells. However, despite this caveat, we believe the results are still conclusive.

CD25$^-$ Tfr Cells Are Stably Foxp3-Expressing Suppressive Treg Cells. Gene expression results suggested that CD25$^-$ Tfr cells might retain suppressive Treg characteristics. To confirm this point, we used an in vitro assay to examine the ability of Treg/Tfr cells to suppress the up-regulation of IgG1 by B cells in culture with Tfh cells. Here, we found that nTreg, eTreg, CD25$^+$ Tfr, and CD25$^-$ Tfr cells all possessed the ability to suppress B-cell switching to IgG1 (Fig. S4*A*) and reduced IgG1 concentrations in the supernatants of the same cultures (Fig. 5*A*). We also used Tfh cells as a negative control for suppressive function. Here, we found that both CD25$^+$ Tfr and CD25$^-$ Tfr cells retained their suppressive function, although this suppressive function was slightly reduced in CD25$^-$ Tfr cells (Fig. S4*B*).

How CD25$^-$ Tfr cells down-regulate CD25 expression is another critical point. In Tfh cells, the transcription factor ASCL2 has been described as both enhancing CXCR5 expression and down-regulating CD25 in Foxp3$^-$ effector T cells (23). CD25$^-$ Tfr cells showed increased expression of ASCL-2 in comparison to other Treg cells (Fig. S3*B*), suggesting that ASCL2 may play a role in their loss of CD25 expression. To address this possibility, we transfected naive CD25$^+$CD62L$^+$ Treg cells with retrovirus containing either empty vector (EV) or ASCL2. We found that ASCL2-transfected cells, but not EV- transfected cells, both marked by NGF-receptor positivity, substantially up-regulated CXCR5 (Fig. 5*B*). Additionally, EV cells did not show a clear change in CD25 expression, whereas ASCL2-transfected cells showed down-regulation of CD25 expression.

IL-2 is well described as a critical factor for the survival and stability of Treg cells, and some CD25-deficient Treg cells have been reported to be unstable transient expressers of Foxp3 (24). This finding poses an important question of how CD25$^-$ Tfr cells are able to survive without IL-2 signaling and whether they are stable Foxp3-expressing cells. In the absence of IL-2, IL-4 has been demonstrated to be able to sustain both Treg proliferation and the suppressive activity of Treg cells (25, 26). Additionally, IL-4 is produced by GC-Tfh cells, suggesting that it would be available in the GC (27). We therefore cultured purified Tfr cells in vitro with anti-CD3/CD28 Dynabeads, with/without IL-2 or IL-4, to test their survival and stability of Foxp3 expression, and we found that CD25$^-$ Tfr and CD25$^+$ Tfr cells were able to retain Foxp3 expression at least as well as nTreg and eTreg cells (Fig. 5*C*, *Left*). Tfh cells did not express Foxp3 in these conditions. Because IL-6 reportedly destabilizes Foxp3 expression (28) but has a role in Tfh formation, IL-6 was added to cell cultures to test the stability of the Treg subsets in adverse conditions. A partial loss of Foxp3 expression was seen; however, the most affected subset was nTreg cells. This finding suggests that CD25$^-$ Tfr and CD25$^+$ Tfr cells are both firmly imprinted into the Treg-cell lineage (Fig. S4*C*). In the absence of cytokine support, nTreg, eTreg, CD25$^+$ Tfr, and CD25$^-$ Tfr cells all survived poorly. The addition of either IL-2 or IL-4 was able to restore survival, although IL-2 was more effective (Fig. 5*C*, *Right*).

During in vitro culture, CD25$^-$ Tfr cells rapidly regained expression of CD25 in the presence or absence of IL-2 or IL-4 (Fig. 5*C*), despite having been confirmed as CD25^{lo} after sorting (Fig. S4*D*). CD25 up-regulation was also seen by Tfh cells themselves, suggesting that once removed from their specialized in vivo microenvironment, both Tfh and Tfr cells may fail to maintain low CD25 expression. Moreover, when CD25$^-$ Tfr and nTconv cells were transferred into athymic nude mice, the CD25$^-$ Tfr cells were largely converted to CD25$^+$CXCR5$^-$ Treg cells (Fig. S4*E*).

Another gold standard marker of Treg-cell lineage is their epigenetic status. Assessing sorted cells for demethylation, we found that CD25$^-$ Tfr and CD25$^+$ Tfr cells both had a demethylated Foxp3 CNS2 region (29) (Fig. 5*D*). This finding is of particular relevance because Foxp3 CNS2 has been described to be responsible for maintaining the stability of Foxp3 expression in the absence of IL-2 and the presence of inflammatory cytokines, such as IL-4 (30, 31).

A number of investigative groups have addressed the possibility that Tfr cells are derived from Tfh cells and have concluded that they are not (7, 8, 10), at least in the absence of incomplete Freund's adjuvant (IFA) (32). However, they did not specifically examine CD25$^-$ Tfr cells, leaving open the question of whether CD25$^-$ Tfr cells are derived from CD25$^+$ nTreg cells. To address this issue, we transferred CD45.2$^+$CD62L$^+$CD25$^+$Foxp3-Gfp$^+$ nTreg cells into athymic nude mice, together with CD45.1$^+$CD62L$^+$CD25$^-$ Tconv cells. Once transferred, Tfh cells and GCs were detectable and CD45.2$^+$Foxp3-Gfp$^+$PD1$^+$CXCR5$^+$ Tfr cells could be seen to contain a fraction of CXCR5^{hi}CD25^{lo}CD25$^-$ Tfr cells (Fig. 5*E*),

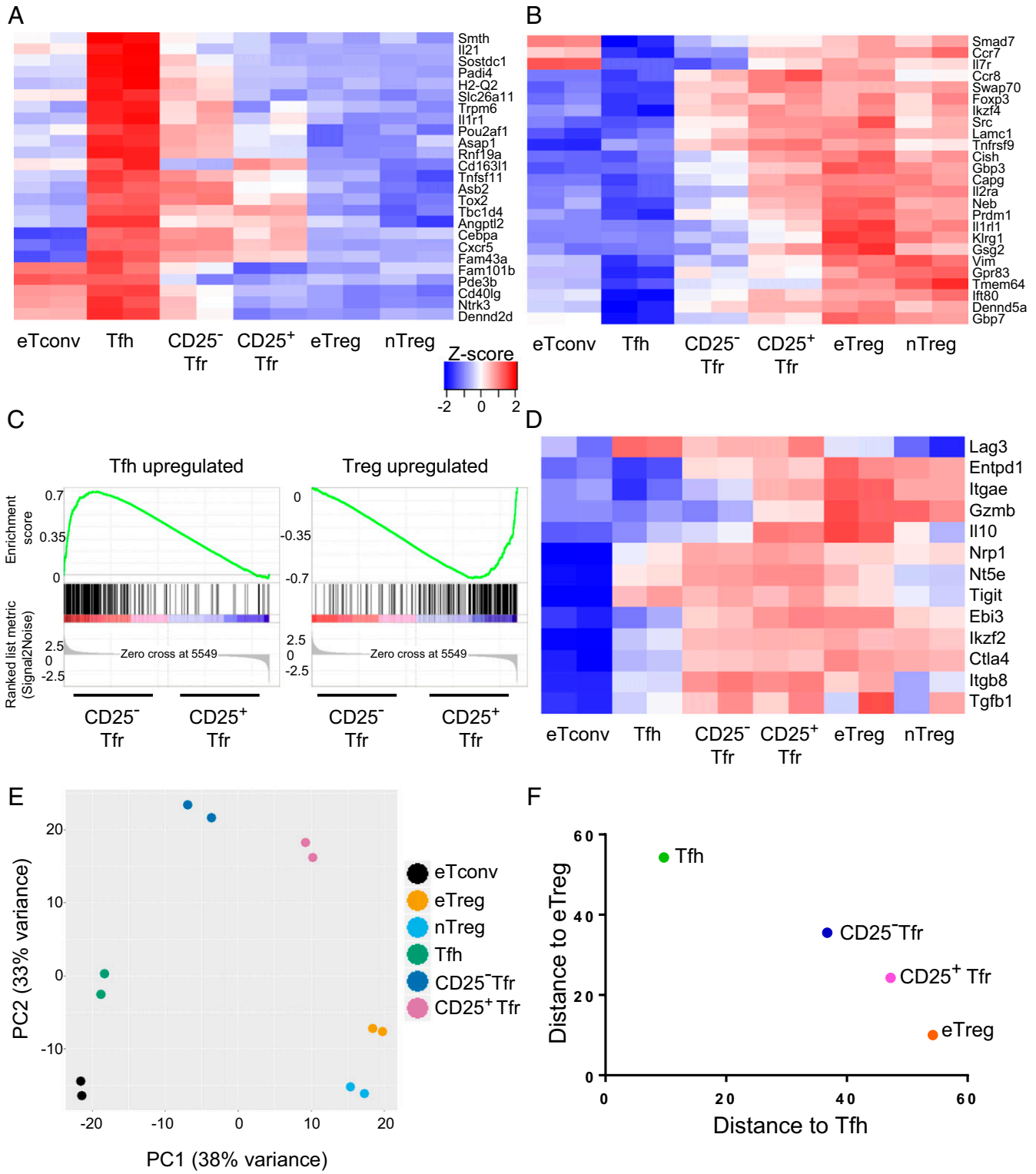

Fig. 4. RNA-Seq of CD25⁻ Tfr cells. Mice were vaccinated with NP-Ova in alum, and dLNs were taken at day 7. A total of 1×10^4 cells were sorted by Becton Dickinson (BD) FACSAria-SORP before RNA-Seq. RNA was extracted using RLT buffer (Qiagen), and then subjected to library preparation using the Quartz-Seq protocol and sequenced by Ion Proton (Life Technologies). Heat maps, principal component analysis, and Euclidean distance analysis were produced using R software. Differential gene expression analysis was performed in R by TCC/DEseq2. Genes with a false discovery rate of <0.01 and a fold change of ≥2 were considered DE. *Z*-scored heat maps of the top 25 up-regulated (*A*) and top 25 down-regulated (*B*) Tfh genes are shown. (*C*) GSEA of CD25⁻ Tfr cells vs. CD25⁺ Tfr cells with a Tfh vs. eTreg DE gene list. Positive enrichment shows enrichment in CD25⁻ Tfr cells, and negative enrichment shows enrichment in CD25⁺ Tfr cells. (*D*) *Z*-scored heat map of selected Treg suppressor genes. (*E*) Principal component (PC) analysis (top 500 most variable genes). (*F*) Euclidean distance to Tfh or eTreg gene expression profile.

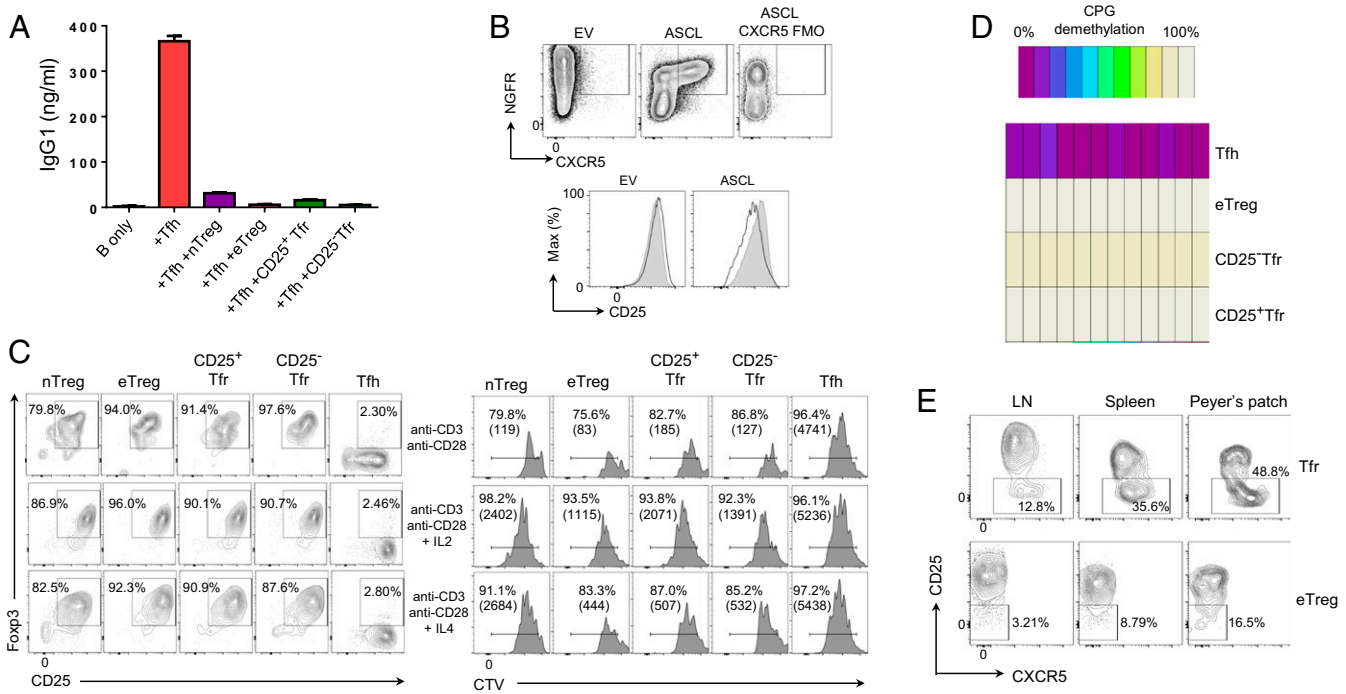

Fig. 5. Suppressive function and stability of CD25$^-$ Tfr cells. Mice were vaccinated with NP-Ova in alum, and dLNs were taken at day 7. Cells were sorted by BD FACSAria-SORP after negative selection of CD4 by magnetic beads. (*A*) Total of 1×10^4 B cells were cultured in the presence of 0.5 μg/mL anti-CD3 and 10 μg/mL anti-IgM, and 5×10^3 Tfh cells were cultured with/without 5×10^3 of the indicated Treg population for 6 d. (*A*) Supernatant IgG1 concentrations were determined by ELISA. Mean ± SEM of duplicates. Data are representative of two separate experiments. (*B*) Total of 1×10^5 nTreg cells were transfected with retrovirus containing EV or ASCL2 by spinfection with viral supernatants, and then cultured in the presence of anti-CD3, anti-CD28 Dynabeads, and 100 U/mL IL-2 for 72 h. CXCR5 expression (*Upper*) and CD25 expression (*Lower*) are shown. The filled histogram is NGFR$^-$, and the clear histogram is NGFR$^+$. Data are representative of three separate experiments. (*C*) Total of 2.5×10^3 purified cells were stained with CellTrace Violet (CTV) and incubated with anti-CD3, anti-CD28 Dynabeads alone (top row), Dynabeads with 100 U/mL IL-2 (middle row), or 20 ng IL-4 (bottom row) for 3 d. (*Left*) Foxp3-GFP and CD25 expression. (*Right*) Proliferation and total cell number (in parentheses) of indicated populations. Data are representative of two separate experiments. (*D*) Total of 1×10^4 cells were assessed for DNA demethylation by bisulfide sequencing. Data are representative of two separate experiments. (*E*) Total of 1×10^6 CD62L$^+$CD25$^-$ nTconv cells from CD45.1 BALB/c mice and 1×10^5 CD62L$^+$CD25$^+$Foxp3$^-$GFP$^+$ nTreg cells from CD45.2 BALB/c eFox mice were transferred i.v. into athymic BALB/c nude mice. One day later, mice were vaccinated, and dLNs, spleens, and Peyer's patches were collected at day 14. CD25 and CXCR5 expression by eTreg cells (Foxp3$^+$CD44$^+$CD62L$^-$CXCR5$^-$) and Tfr cells (Foxp3$^+$CD44$^+$CD62L$^-$CXCR5$^+$PD1$^+$) is shown. Data are pooled from three mice, representative of two separate experiments.

demonstrating that CD25$^+$ nTreg cells were able to give rise to CD25$^-$ Tfr cells. As before, the proportion of these cells varied by lymphoid organs, with the spleen and Peyer's patches having higher proportions of CD25$^-$ Tfr cells. Loss of CD25 expression was specific to Tfr cells because eTreg cells had significantly smaller fractions of CD25$^-$ cells (Fig. 5*E*). CD45.2$^-$Foxp3$^+$Foxp3-Gfp$^-$ cells (which express Foxp3 protein but lack the Foxp3-Gfp gene) converted from transferred Tconv cells were largely absent from both CD25$^+$ Tfr and CD25$^-$ Tfr cells. (Fig. S4*F*).

IL-2 Antagonizes the Formation and Maintenance of CD25$^-$ Tfr Cells. To assess the impact of the loss of IL-2 on Tfr-cell formation, we examined IL-2–deficient mice. Here, we found that the proportions of Treg cells were significantly reduced (Fig. S5*A*), coinciding with large-scale spontaneous formation of Tfh cells and GCs (Fig. S5*B*). Of the remaining Treg cells, a large proportion were CXCR5$^+$PD1$^+$CD25$^-$ Tfr cells, confirming their lack of dependence on IL-2 signaling (Fig. S5*C*). Although homozygous IL-2 KO ($^{-/-}$) mice suffer from severe inflammation, heterozygous ($^{+/-}$) mice were healthy at the age used in these experiments and showed similar, if less dramatic, results. Although the numbers of Tfr cells were very low in unvaccinated wild-type or heterozygous mice, we assessed Tfr cells in the Peyer's patches and found that the percentage of CD25$^-$ Tfr cells was increased in both the IL-2 KO$^{-/-}$ and IL-2/KO$^{+/-}$ mice (Fig. S5*D*). In addition, in vivo IL-2 blockade by antibody enhanced the formation of CD25$^-$ Tfr and Tfh cells while reducing Treg-cell frequencies (Fig. S5 *E*–*G*).

To address the effect of adding IL-2, we used IL-2/anti–IL-2 complexes that have been demonstrated to expand Treg cells efficiently in vivo (33). Because the spleen contained a relatively large proportion of CD25$^-$ Tfr cells (Fig. S1), we used the spleen for assessing the effects of IL-2/anti–IL-2 complexes and found that Foxp3$^+$ cells rapidly expanded in a dose-dependent manner over the course of a week, whereas Tfr cells were reduced (Fig. S6 *A* and *B*). The remaining Tfr cells became CD25$^+$ (Fig. S6 *A* and *B*), although they also lost expression of BCL6 (Fig. S6*C*). CD25$^-$ Tfr cells were reduced in total number as well as proportion, demonstrating that this result was not simply a dilution effect due to excessive eTreg-cell proliferation (Fig. S6*C*). Some of these effects may be indirect due to the impact of IL-2 on Tfh cells and GCs, which were both reduced by the treatment (Fig. S6*C*). In the Peyer's patches, CD25$^-$ Tfr cells were also significantly reduced in frequency, but the reduction in number was not significant ($P = 0.08$), whereas GCs and Tfh were retained, suggesting that the effects could not be ascribed to loss of GCs but that preferential expansion of CD25$^+$ Treg cells may be a factor (Fig. S6 *D* and *E*). We also took advantage of a published dataset examining CD25^{hi} and CD25^{lo} Treg cells from wild-type mice, as well as Treg cells from IL-2$^{-/-}$ mice with/without i.p. injection of IL-2. As predicted by our results, CD25^{lo} Treg cells had enhanced expression of *Cxcr5*, *Bcl6*, and *Pdcd1* (Fig. S6*F*). Furthermore, Treg cells from IL-2–deficient mice had similar up-regulation of these genes, and this up-regulation was rapidly diminished by IL-2 treatment, which caused down-regulation of *Cxcr5*, *Bcl6*, and *Pdcd1* but up-regulation of *Il2ra* and *Selplg* (PSGL-1) (12) (Fig. S6*F*) [Gene Expression Omnibus (GEO) database accession no. GSE4179].

Additionally, GSEA analysis comparing RNA-Seq data from our CD25$^-$ Tfr and CD25$^+$ Tfr cells with the RNA-Seq data of Treg cells from IL2Rβ KO mice demonstrated that CD25$^+$ Tfr cells were significantly enriched for the genes down-regulated by IL2Rβ KO Treg cells compared with wild-type Treg cells (34) (Fig. S6*G*). CD25$^-$ Tfr enrichment of the UP signature was not statistically significant.

Human Tfr Cells in the Blood and Tonsils. Although murine Tfr cells are relatively well characterized, comparatively little is known about human Tfr cells. We examined human peripheral blood mononuclear cells (PBMCs) from healthy donors and assessed their expression of the Tfh marker CXCR5 within Treg cells. We first gated CD3$^+$CD4$^+$CD19$^-$CD8$^-$CD14$^-$ T cells into CD45RA$^+$ naive and CD45RA$^-$ effector fractions. Here, we found that within CD45RA$^-$ T cells, Foxp3$^-$CXCR5$^+$ Tfh and Foxp3$^+$CXCR5$^+$ Tfr cells could be clearly separated (Fig. 6*A*). As such, we defined the CD45RA$^-$ populations as follows: CXCR5$^+$Foxp3$^+$ circulating Tfr (cTfr) cells, CXCR5$^+$Foxp3$^-$ cTfh cells, CXCR5$^-$Foxp3$^-$ eTconv cells, and CXCR5$^-$Foxp3$^+$ eTreg cells. The nTreg and nTconv cells were gated as CD45RA$^+$Foxp3$^+$ and CD45RA$^+$Foxp3$^-$, respectively. The cTfr, eTreg, and nTreg cells were all CD25$^+$Helios$^+$CD127^{lo} (Fig. 6*A*). The cTfr cells were then sorted (CD127^{lo}CD25$^+$ was used in place of Foxp3) and further confirmed as bona fide Treg cells with demethylation of Foxp3 CNS2 (Fig. 6*B*).

In comparison to eTreg cells, cTfr cells had reduced expression of Foxp3, and the previously identified eTreg marker CD15s (35) (Fig. 6*C*). However, although expression was reduced in comparison to eTreg cells, it was increased in comparison to nTreg cells. There was not a clear CD25$^-$ population, but the level of CD25 expression was significantly decreased in cTfr cells in comparison to both eTreg and nTreg cells, suggesting that in contrast to eTreg cells, Tfr down-regulated CD25 on activation. We also assessed markers of activation and proliferation (HLA-DR and Ki-67) and found that cTfr cells had low levels of these markers in comparison to eTreg cells (Fig. S7*A*). Because we have previously demonstrated that positivity for CD15s and high levels of Foxp3^{hi} expression are associated with Treg-suppressive function (36), this finding raised the question of whether cTfr cells retained their suppressive function. In vitro, both eTreg and cTfr cells lacked any helper function to support B-cell survival or antibody production (Fig. S7 *B* and *C*) but were able to suppress in vitro B-cell activation by Tfh cells, blocking formation of CD20^{lo}CD38^{hi} plasma cells and the resulting IgG production (Fig. 6*D* and Fig. S7*C*). Additionally, in terms of ability to suppress T-cell proliferation, we found that in vitro, cTfr cells possessed suppressive function similar to the suppressive function of nTreg cells: higher than Tfh cells but less than highly activated eTreg cells (Fig. S7*D*). To provide a more detailed assessment of cTfr cells, we then performed RNA-Seq. Similar to the results seen in mice (Fig. 4*F* and Fig. S3*D*), we found that cTfr cells had levels of overall Euclidean distance of their gene expression signature similar to both eTreg and Tfh cells, although hierarchical clustering revealed that they were slightly closer to Tfh cells than eTreg cells, suggesting an intermediate genotype (Fig. 6*E*). This finding was also confirmed by heat maps of the 25 most up-regulated and down-regulated genes from Tfh to eTreg cells, with cTfr cells proven to be intermediates (Fig. 6*F* and Dataset S2). To explore the unique gene expression profile of cTfr cells further, fold change and expression of all genes between cTfr and Tfh cells (Fig. 6*G*, *Left*) or between cTfr and eTreg cells (Fig. 6*G*, *Right*) were plotted with DE genes [$\log_2$-fold change >1, q value (adjusted P) <0.05] highlighted in red. In comparison to Tfh cells, the cTfr UP signature was characterized by many of the genes associated with Treg function, such as Foxp3, IL2RA (CD25), and PRMD1 (Blimp-1); in contrast, few genes were down-regulated. In comparison to eTreg cells, the cTfr UP signature was characterized by gain of Tfh-related molecules and transcription factors, such as CXCR5, TCF7, and POU2AF1. We have previously demonstrated that POU2AF1 is up-regulated in blood Tfh cells, particularly the highly active CXCR3$^-$PD1$^+$CXCR5$^+$ subset (37). Here, we found that POU2AF1 was in the UP signature of cTfr cells in comparison to both Tfh and eTreg cells, suggesting that it might have a particular role in Tfr cells. The activation marker CD38 was also up-regulated in cTfr cells in comparison to both Tfh and eTreg cells. In comparison to eTreg cells, the cTfr DOWN signature contained many of the same genes seen in the UP signature in comparison to Tfh cells, such as FOXP3, IL2RA, and PRDM1, confirming their intermediate expression level by cTfr cells. Additionally, chemokine receptors and Treg activation markers, such as CCR4, CCR8, CCR10, and components of HLA-DR, were down-regulated. Other critical Treg markers/suppressive molecules, such as IKZF2 (Helios), IKZF4 (Eos), and CTLA-4, were not DE by cTfr cells in comparison to eTreg cells. Full lists of all DE genes are given in Dataset S2.

Although cTfr cells are CD25^{lo}, they cannot be considered the direct equivalents of murine CD25– Tfr cells located in GCs. To address the phenotype of human Tfr cells in GCs, we used tonsillar samples. Because we had found that most circulating Treg cells expressed Helios, Treg cells were gated as Helios$^+$Foxp3$^+$ cells to differentiate them from highly activated non-Treg cells in this environment. Tonsillar Tfh cells have previously been shown to be subdivided into Tfh and GC-Tfh cells based on the expression of CXCR5, PD1, and BCL6. Because nothing was known about CD25$^-$ Tfr cells in humans, we used a conservative gating strategy based on these known Tfh populations. We defined Tconv cells as CXCR5$^-$ BCL6$^-$, Tfh cells as CXCR5$^+$BCL6^{lo}, and GC-Tfh cells as CXCR5^{hi} BCL6^{hi} (Fig. 7*A*) before using the same gates applied to the Foxp3$^+$ Helios$^+$ population to identify eTreg, Tfr, and CD25$^-$ Tfr cells, which made up 4.95% (±0.87 SEM, n = 6) of Foxp3$^+$Helios$^+$ Treg cells. Here, we found that, similar to mouse CD25$^-$ Tfr cells, human CD25$^-$ Tfr cells were BCL6^{hi}CXCR5^{hi}PD1^{hi}Helios$^+$Foxp3$^+$CD25$^-$ (Fig. 7 *B* and *C*). Helios$^-$Foxp3$^+$ cells contained a large fraction of CXCR5 intermediate cells but lacked a CXCR5^{hi}BCL6^{hi} population and were broadly similar in phenotype to Helios$^+$CXCR5$^+$BCL6^{lo} Tfr cells (Fig. 7*C* and Fig. S7*E*). We supplemented manual gating with ACCENSE, using CXCR5, PD1, BCL6, and CD25 to map Foxp3$^+$Helios$^+$-gated cells, and then K-means clustering to identify separate regions automatically (Fig. S7*F*). K-means clustering was indeed able to identify a BCL6^{hi}PD1^{hi}CD25^{lo} region of cells that corresponded to the manually gated CD25$^-$ Tfr cells (Fig. S7*G*), confirming the robustness of the manual analysis.

Discussion

Here, we have demonstrated that in contrast to other Treg cells, CD25$^-$ Tfr cells are expanded in the absence of IL-2 and are reduced by its presence. In humans, cTfr cells are CD25^{lo}, whereas BCL6^{hi}CXCR5^{hi}PD1^{hi} Tfr cells in the tonsils are CD25$^-$. In many cases, CD25$^-$ Tfr cells down-regulate eTreg markers, but this down-regulation must be viewed in the context that they still maintain higher expression levels than either nTreg or non-Treg cells. RNA-Seq analysis also identifies that CD25$^-$ Tfr cells have an overall gene expression signature as similar to Tfh cells as to eTreg cells. However, despite this finding, they maintain expression of key Treg-associated genes and were derived from CD25$^+$ nTreg cells. Together with their maintenance of suppressive function, demethylation of Foxp3 CNS2, and stable expression of Foxp3, this finding allows CD25$^-$ Tfr cells to be unambiguously identified as a Treg subpopulation. It is also important to note that in human tonsils, CD25$^-$ Tfr cells are the only Foxp3-expressing population that expresses significant amounts of BCL6.

We noted that the ratio of CD25-expressing Tfr cells varied between lymphoid organs. This variation may be due to availability of STAT5 signaling, because a lower proportion of Treg cells are pSTAT5$^+$ in the spleen than in the LNs (38). IL-2–driven pSTAT5$^+$ clusters of Treg cells are primarily found in the T-cell zones of lymphoid organs, demonstrating the paucity of IL-2 availability in the B-cell follicles (38, 39).

Loss of CD25 is an enrichment marker for GC localization, but some Tfr cells in the B-cell follicle are also CD25$^{-/lo}$; additionally CD25$^-$ Tfr cells are capable of reexpressing CD25 on in vitro stimulation. As such, CD25$^-$ Tfr cells are best thought of as a mature stage of Tfr differentiation that is enriched for, but not

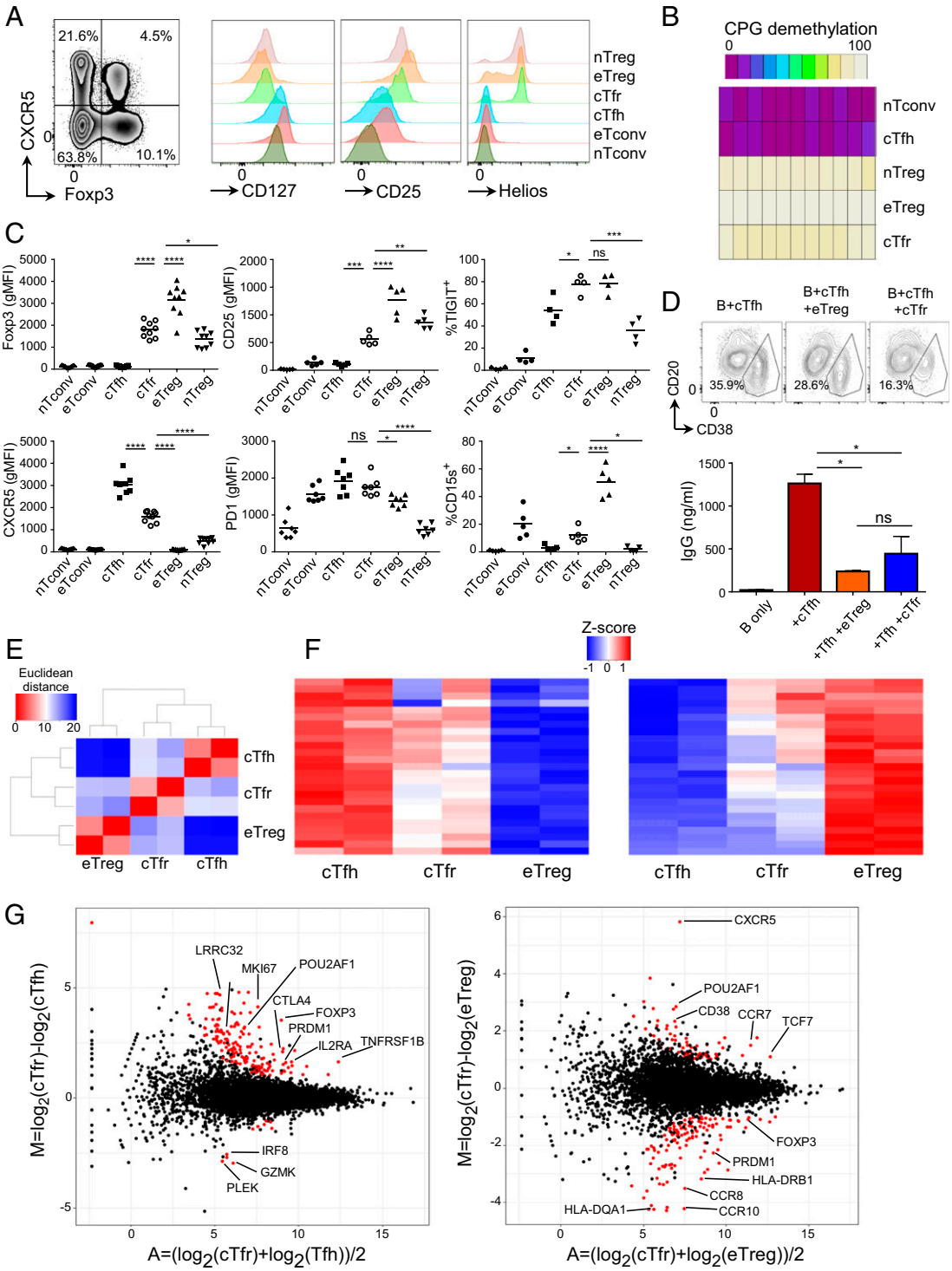

Fig. 6. Human circulating Tfr cells. PBMCs were purified from the blood of healthy donors. (*A*) Zebra plot of Foxp3 and CXCR5 expression by $CD4^+CD3^+$ $CD45RA^-$ T cells (*Left*) and histograms of CD127, CD25, and Helios expression by the indicated populations (*Right*), representative of more than five (*Left*) and two separate (*Right*) experiments, respectively. (*B*) Total of 1×10^4 cells were sorted by BD FACSAria-SORP after negative selection of CD4 by magnetic beads as $CD45RA^+CD127^+CD25^-$ nTconv cells, $CD45RA^-CD127^+CD25^-CXCR5^+$ cTfh cells, $CD45RA^+CD127^{lo}CD25^+$ nTreg cells, $CD45RA^-CD127^{lo}CD25^+CXCR5^-$ eTreg cells, and $CD45RA^-CD127^{lo}CD25^+CXCR5^+$ cTfr cells, and methylation status was assessed by bisulfide sequencing. Data are representative of two separate experiments. (*C*) Summary data of protein expression by indicated populations. Data are pooled from four to nine mice, representative of two to four separate experiments. (*D*) Total of 5×10^4 B cells were cultured in the presence of anti-CD3 and anti-CD28 Dynabeads with/without 1×10^4 cTfh cells and/or 1×10^4 eTreg cells or cTfr cells for 6 d. $CD20^{lo}CD38^{hi}$ plasma cell formation (*Upper*) and IgG concentration in supernatants determined by ELISA (*Lower*) are shown (mean ± SEM of duplicates). Data are representative of two separate experiments. (*E–G*) Total of 1×10^4 cells were sorted by BD FACSAria-SORP as in *B* before RNA-Seq. Heat maps, principal component analysis, and Euclidean distance analysis were produced using R software. Differential gene expression analysis was performed in R by TCC/DEseq2. Genes with a false discovery rate of <0.05 and a fold change of ≥2 were considered DE. (*E*) Euclidean distance analysis of whole-gene expression profile. (*F*) *Z*-scored heat maps of the top 25 up-regulated (*Left*) and the top 25 down-regulated (*Right*) Tfh genes. (*G*) Plots of $\log_2$-fold change (M) and gene expression (A) between cTfr and Tfh cells (*Left*) or cTfr and eTreg cells (*Right*). DE genes are highlighted in red (*$P \leq 0.05$, **$P \leq 0.01$, ***$P \leq 0.001$, ****$P \leq 0.0001$). ns, not significant.

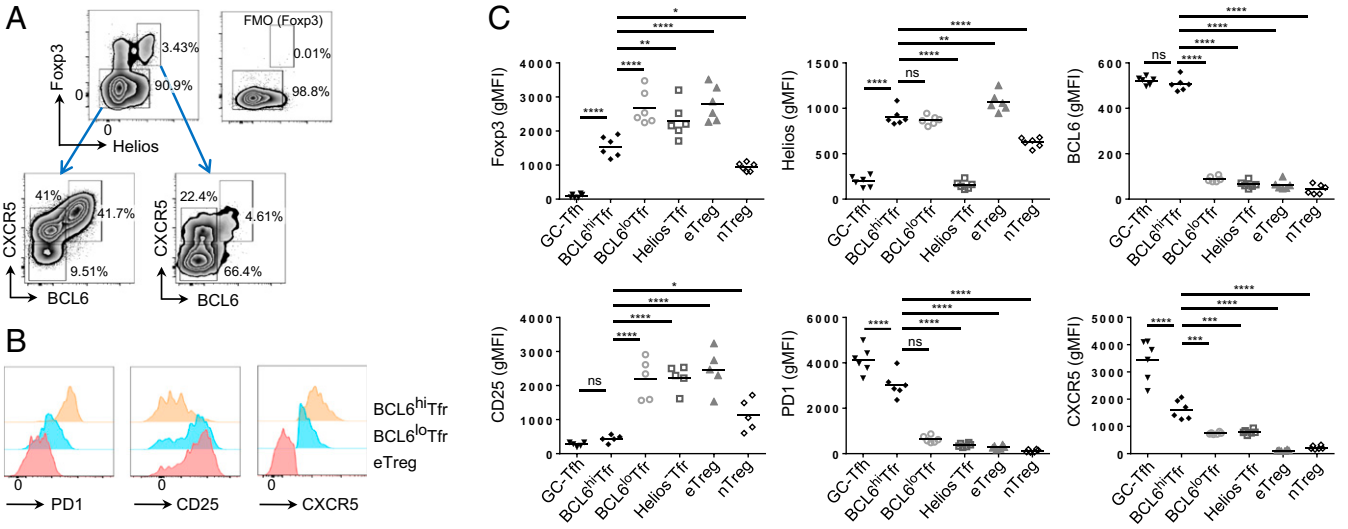

Fig. 7. Human tonsillar Tfr cells. (*A–C*) Fresh human tonsils were obtained from the National Disease Resource Interchange. (*A*) CD45RA$^-$CD4$^+$CD3$^+$B220$^-$ gated cells were then further dissected to CXCR5$^-$BCL6$^-$ Foxp3$^+$ as eTreg cells, CXCR5$^+$BCL6^{lo}Foxp3$^-$ as Tfh cells, CXCR5$^+$BCL6^{lo}Foxp3$^+$Helios$^+$ as BCL6^{lo} Tfr cells or Helios$^-$ Tfr cells (when Helios$^-$), and CXCR5$^+$BCL6^{hi} as GC-Tfh (when Foxp3$^-$) or BCL6^{hi} Tfr cells (when Foxp3$^+$). (*Upper Right*) Foxp3 FMO staining is shown. (*B*) Expression of PD1, CD25, and CXCR5 by indicated populations. (*C*) Summary data of indicated marker expression. Data are pooled from six mice, representative of two separate experiments (*$P \leq 0.05$, **$P \leq 0.01$, ****$P \leq 0.0001$). ns, not significant.

necessarily made entirely of, cells in the GC. This caveat may also be the case with current strategies used to separate Tfh cells from GC-Tfh cells, with the CXCR5^{hi}PD1^{hi}BCL6^{hi} phenotype associated with GC-Tfh cells being enriched for, but not exclusive to, GC localized cells, as confirmed by several microscopy studies (18, 40). Additionally, GC-Tfh cells are capable of cycling in and out of the GCs, so they may not be localized in the GC at all times (18). Further study is needed to assess if Tfr cells also cycle in this manner.

It has recently been demonstrated that CD25 is down-regulated by a subset of CD103$^+$, KLRG1$^+$, and CXCR3$^+$ eTreg cells preferentially located in the nonlymphoid tissues (39). These cells lose access to IL-2 signaling in the T-cell zones and are sustained by ICOS signaling but, in contrast to CD25$^-$ Tfr cells, only partially lose CD25 expression. This finding demonstrates that loss of dependence on IL-2 signaling may be a common feature of several eTreg subsets (39), although antagonism by IL-2 may be unique to CD25$^-$ Tfr cells. Additionally, given the high level of ICOS expression by Tfr cells and the relative abundance of ICOS-ligand in the GC environment, it seems likely that ICOS, in addition to IL-4, may have a role in the survival of CD25$^-$ Tfr cells.

Despite down-regulation of some eTreg-associated genes, CD25$^-$ Tfr cells maintained their expression of the majority of suppressive molecules, most critically CTLA-4, which we and others have demonstrated to have a key role in Tfr-dependent control of Tfh function (41–43). Notably many of the genes down-regulated in CD25$^-$ Tfr cells, such as *Klrg1*, *Itgae* (CD103), *Prdm1* (BLIMP-1), *Il10*, and *Gzmb* (Granzyme B), are IL-2–dependent (34). Together with the known importance of IL-2 receptor signaling in the development of KLRG1$^+$BLIMP-1^{hi} eTreg cells (17, 34), this finding suggests that CD25$^-$ Tfr cells have primarily lost the IL-2–dependent component of eTreg gene expression. We found that ASCL2 may have a role in the down-regulation of CD25; additionally, a recent report has demonstrated that IL-21 signaling in Tregs inhibits CD25 expression via BCL6 (44).

The relative in vivo importance of CD25$^-$ Tfr cells as opposed to CD25$^+$ Tfr cells remains to be demonstrated due to the difficultly of directly manipulating CD25$^-$ Tfr cells without affecting CD25$^+$ Tfr cells. However, given their GC localization and maintenance of suppressive capacity, it is reasonable to expect that CD25$^-$ Tfr cells are the primary suppressive cells in established GCs, whereas CD25$^+$ Tfr cells are a precursor population and may also be involved in regulation of the earlier stages of B-cell responses.

Our results suggest that the antagonism between BLIMP-1 and BCL6 may cause two main differentiation paths for eTreg cells, that is, a classical IL-2–dependent path defined by BLIMP-1 and characterized by expression of CD25, KLRG1, CD103, Granzyme B, and IL-10, and a separate IL-2–antagonized path defined by BCL6 and characterized by CXCR5, TIGIT, ICOS, BTLA, and PD1. This finding adds a layer of complexity when assessing the phenotype of Treg cells, because assessment of total Treg cells may fail to differentiate between changes in activation status and subpopulations. For example, expression levels of CD103 could be determined by either overall changes to Treg activation status or underlying shifts in compositions of eTreg subpopulations that do or do not favor CD103. Because simultaneous identification of all Treg subpopulations is impractical, characterization and use of subpopulation-independent Treg activation markers, such as Ki-67, CD44, and CTLA-4, and loss of CCR7 and CD62L may potentially be more appropriate for a broad overview of Treg activation status.

Tfr cells maintain a delicate balance between incompatible aspects of their Tfh and Treg identities. We propose that in both mice and humans, CD25$^-$ Tfr cells down-regulate CD25 to insulate themselves from IL-2 signaling that would otherwise lead to up-regulation of BLIMP-1 and prevent high-level expression of BCL6 and other Tfh factors. This down-regulation allows the cells to traffic to the inner follicles and GCs. Although some aspects of Treg gene expression are lost or partially down-regulated, key features, such as Foxp3, GITR, Helios, and CTLA-4 expression, are retained. This finding demonstrates that Tfr cells display high levels of flexibility to adopt large portions of the Tfh gene signature while still retaining their fundamental identity as Treg cells.

Materials and Methods

Detailed methods can be found in *Supporting Information*.

Murine Sample Preparation. BALB/c and C57BL/6 mice were obtained from CLEA Japan, Inc. and maintained under specific pathogen-free conditions. All experiments used mice on a C57BL/6 background except where noted. BCL6 flox, IL-2$^{-/-}$, BLIMP-1 reporter, Foxp3 fusion protein DTR-GFP (FDG), Foxp3-Gfp eFox, and IL-21 reporter mice have already been described (45–49).

Mice were killed by CO^2, and draining LNs (inguinal), spleens, and/or Peyer's patches were removed by dissection before disaggregation by grinding with frosted glass slides and suspension in RPMI media and 2% FCS.

Spleens were further treated with red cell lysis buffer (Sigma). Murine experiments were conducted with age- and sex-matched littermates of at least 6 wk of age, except where noted, and were conducted in compliance with Osaka University regulations.

Human Sample Preparation. PBMCs were isolated from the blood of healthy donors by density gradient centrifugation with Ficoll–Paque (GE Healthcare). Fresh human tonsils were obtained from the National Disease Resource Interchange. The protocol was approved by the La Jolla Institute Institutional Review Board. Tonsil preparation was carried out as previously described elsewhere (50). All blood donors provided written informed consent before sampling, according to the Declaration of Helsinki. This study was approved by the Osaka University Research Ethics Committee.

Statistics. Comparisons between groups were calculated by an unpaired Student's *t* test for a single comparison or by ANOVA plus a Holm–Sidak *t* test for multiple comparisons (*$P \leq 0.05$, **$P \leq 0.01$, ***$P \leq 0.001$, ****$P \leq 0.0001$). All statistics were calculated by GraphPad Prism V6.07 (GraphPad Software). Outliers were defined and excluded on the basis of the Grubbs outlier test (α value of 0.01); a single outlier was removed from Fig. S6 (indicated in legend), but no other outliers were identified.

ACKNOWLEDGMENTS. We thank Steven Nutt for provision of BLIMP-1 reporter mice; Masato Kubo for provision of IL-21 reporter mice; K. Teshima, Y. Nakamura, T. Iida, and H. Rain for technical support; and Z. Mikulski for assistance with human tonsils. Bioinformatics analyses were conducted using the computer system at the Genome Information Research Center, Research Institute for Microbial Diseases, Osaka University. This study was supported by Japan Society for the Promotion of Science (JSPS) Grants-in-Aid for Scientific Research (A Grant 26253030 to S.S. and B Grant 16H05181 to C.C.), a JSPS Grant-in-Aid for Young Scientists (B Grant 15K19129 to J.B.W.), the Novartis Foundation (Japan) for the Promotion of Science (Grant 15-123 to J.B.W.), and the Japan Agency for Medical Research and Development (Grant 16ak0101010h0205 to C.C.).

1. Crotty S (2014) T follicular helper cell differentiation, function, and roles in disease. *Immunity* 41:529–542.
2. Johnston RJ, et al. (2009) Bcl6 and Blimp-1 are reciprocal and antagonistic regulators of T follicular helper cell differentiation. *Science* 325:1006–1010.
3. Nurieva RI, et al. (2009) Bcl6 mediates the development of T follicular helper cells. *Science* 325:1001–1005.
4. Yu D, et al. (2009) The transcriptional repressor Bcl-6 directs T follicular helper cell lineage commitment. *Immunity* 31:457–468.
5. Sakaguchi S, Yamaguchi T, Nomura T, Ono M (2008) Regulatory T cells and immune tolerance. *Cell* 133:775–787.
6. Wing JB, Sakaguchi S (2014) Foxp3$^+$ T(reg) cells in humoral immunity. *Int Immunol* 26:61–69.
7. Chung Y, et al. (2011) Follicular regulatory T cells expressing Foxp3 and Bcl-6 suppress germinal center reactions. *Nat Med* 17:983–988.
8. Wollenberg I, et al. (2011) Regulation of the germinal center reaction by Foxp3+ follicular regulatory T cells. *J Immunol* 187:4553–4560.
9. Sage PT, Sharpe AH (2016) T follicular regulatory cells. *Immunol Rev* 271:246–259.
10. Linterman MA, et al. (2011) Foxp3+ follicular regulatory T cells control the germinal center response. *Nat Med* 17:975–982.
11. Sakaguchi S, Sakaguchi N, Asano M, Itoh M, Toda M (1995) Immunologic self-tolerance maintained by activated T cells expressing IL-2 receptor alpha-chains (CD25). Breakdown of a single mechanism of self-tolerance causes various autoimmune diseases. *J Immunol* 155:1151–1164.
12. Fontenot JD, Rasmussen JP, Gavin MA, Rudensky AY (2005) A function for interleukin 2 in Foxp3-expressing regulatory T cells. *Nat Immunol* 6:1142–1151.
13. Cretney E, et al. (2011) The transcription factors Blimp-1 and IRF4 jointly control the differentiation and function of effector regulatory T cells. *Nat Immunol* 12:304–311.
14. Johnston RJ, Choi YS, Diamond JA, Yang JA, Crotty S (2012) STAT5 is a potent negative regulator of TFH cell differentiation. *J Exp Med* 209:243–250.
15. Ballesteros-Tato A, et al. (2012) Interleukin-2 inhibits germinal center formation by limiting T follicular helper cell differentiation. *Immunity* 36:847–856.
16. Shekhar K, Brodin P, Davis MM, Chakraborty AK (2014) Automatic Classification of Cellular Expression by Nonlinear Stochastic Embedding (ACCENSE). *Proc Natl Acad Sci USA* 111:202–207.
17. Cheng G, et al. (2012) IL-2 receptor signaling is essential for the development of Klrg1+ terminally differentiated T regulatory cells. *J Immunol* 189:1780–1791.
18. Shulman Z, et al. (2013) T follicular helper cell dynamics in germinal centers. *Science* 341:673–677.
19. Poholek AC, et al. (2010) In vivo regulation of Bcl6 and T follicular helper cell development. *J Immunol* 185:313–326.
20. Haynes NM, et al. (2007) Role of CXCR5 and CCR7 in follicular Th cell positioning and appearance of a programmed cell death gene-1high germinal center-associated subpopulation. *J Immunol* 179:5099–5108.
21. Moriyama S, et al. (2014) Sphingosine-1-phosphate receptor 2 is critical for follicular helper T cell retention in germinal centers. *J Exp Med* 211:1297–1305.
22. Kitano M, et al. (2011) Bcl6 protein expression shapes pre-germinal center B cell dynamics and follicular helper T cell heterogeneity. *Immunity* 34:961–972.
23. Liu X, et al. (2014) Transcription factor achaete-scute homologue 2 initiates follicular T-helper-cell development. *Nature* 507:513–518.
24. Miyao T, et al. (2012) Plasticity of Foxp3(+) T cells reflects promiscuous Foxp3 expression in conventional T cells but not reprogramming of regulatory T cells. *Immunity* 36:262–275.
25. Thornton AM, Piccirillo CA, Shevach EM (2004) Activation requirements for the induction of CD4+CD25+ T cell suppressor function. *Eur J Immunol* 34:366–376.
26. Pace L, Pioli C, Doria G (2005) IL-4 modulation of CD4+CD25+ T regulatory cell-mediated suppression. *J Immunol* 174:7645–7653.
27. King IL, Mohrs M (2009) IL-4-producing CD4+ T cells in reactive lymph nodes during helminth infection are T follicular helper cells. *J Exp Med* 206:1001–1007.
28. Barbi J, Pardoll D, Pan F (2014) Treg functional stability and its responsiveness to the microenvironment. *Immunol Rev* 259:115–139.
29. Ohkura N, et al. (2012) T cell receptor stimulation-induced epigenetic changes and Foxp3 expression are independent and complementary events required for Treg cell development. *Immunity* 37:785–799.
30. Feng Y, et al. (2014) Control of the inheritance of regulatory T cell identity by a cis element in the Foxp3 locus. *Cell* 158:749–763.
31. Li X, Liang Y, LeBlanc M, Benner C, Zheng Y (2014) Function of a Foxp3 cis-element in protecting regulatory T cell identity. *Cell* 158:734–748.
32. Aloulou M, et al. (2016) Follicular regulatory T cells can be specific for the immunizing antigen and derive from naive T cells. *Nat Commun* 7:10579.
33. Webster KE, et al. (2009) In vivo expansion of T reg cells with IL-2-mAb complexes: Induction of resistance to EAE and long-term acceptance of islet allografts without immunosuppression. *J Exp Med* 206:751–760.
34. Yu A, Zhu L, Altman NH, Malek TR (2009) A low interleukin-2 receptor signaling threshold supports the development and homeostasis of T regulatory cells. *Immunity* 30:204–217.
35. Miyara M, et al. (2015) Sialyl Lewis x (CD15s) identifies highly differentiated and most suppressive FOXP3high regulatory T cells in humans. *Proc Natl Acad Sci USA* 112:7225–7230.
36. Miyara M, et al. (2009) Functional delineation and differentiation dynamics of human CD4+ T cells expressing the FoxP3 transcription factor. *Immunity* 30:899–911.
37. Locci M, et al.; International AIDS Vaccine Initiative Protocol C Principal Investigators (2013) Human circulating PD-1+CXCR3-CXCR5+ memory Tfh cells are highly functional and correlate with broadly neutralizing HIV antibody responses. *Immunity* 39:758–769.
38. Liu Z, et al. (2015) Immune homeostasis enforced by co-localized effector and regulatory T cells. *Nature* 528:225–230.
39. Smigiel KS, et al. (2014) CCR7 provides localized access to IL-2 and defines homeostatically distinct regulatory T cell subsets. *J Exp Med* 211:121–136.
40. Suan D, et al. (2015) T follicular helper cells have distinct modes of migration and molecular signatures in naive and memory immune responses. *Immunity* 42:704–718.
41. Wing JB, Ise W, Kurosaki T, Sakaguchi S (2014) Regulatory T cells control antigen-specific expansion of Tfh cell number and humoral immune responses via the coreceptor CTLA-4. *Immunity* 41:1013–1025.
42. Sage PT, Paterson AM, Lovitch SB, Sharpe AH (2014) The coinhibitory receptor CTLA-4 controls B cell responses by modulating T follicular helper, T follicular regulatory, and T regulatory cells. *Immunity* 41:1026–1039.
43. Wang CJ, et al. (2015) CTLA-4 controls follicular helper T-cell differentiation by regulating the strength of CD28 engagement. *Proc Natl Acad Sci USA* 112:524–529.
44. Jandl C, et al. (2017) IL-21 restricts T follicular regulatory T cell proliferation through Bcl-6 mediated inhibition of responsiveness to IL-2. *Nat Commun* 8:14647.
45. Lahl K, et al. (2007) Selective depletion of Foxp3+ regulatory T cells induces a scurfy-like disease. *J Exp Med* 204:57–63.
46. Harada Y, et al. (2012) The 3′ enhancer CNS2 is a critical regulator of interleukin-4-mediated humoral immunity in follicular helper T cells. *Immunity* 36:188–200.
47. Kallies A, et al. (2004) Plasma cell ontogeny defined by quantitative changes in blimp-1 expression. *J Exp Med* 200:967–977.
48. Ise W, et al. (2014) Memory B cells contribute to rapid Bcl6 expression by memory follicular helper T cells. *Proc Natl Acad Sci USA* 111:11792–11797.
49. Ito Y, et al. (2014) Detection of T cell responses to a ubiquitous cellular protein in autoimmune disease. *Science* 346:363–368.
50. Kroenke MA, et al. (2012) Bcl6 and Maf cooperate to instruct human follicular helper CD4 T cell differentiation. *J Immunol* 188:3734–3744.
51. Subramanian A, et al. (2005) Gene set enrichment analysis: A knowledge-based approach for interpreting genome-wide expression profiles. *Proc Natl Acad Sci USA* 102:15545–15550.
52. Zhao H, et al. (2014) Olfactory plays a key role in spatiotemporal pathogenesis of cerebral malaria. *Cell Host Microbe* 15:551–563.
53. Sasagawa Y, et al. (2013) Quartz-Seq: A highly reproducible and sensitive single-cell RNA sequencing method, reveals nongenetic gene-expression heterogeneity. *Genome Biol* 14:R31.
54. Sun J, Nishiyama T, Shimizu K, Kadota K (2013) TCC: An R package for comparing tag count data with robust normalization strategies. *BMC Bioinformatics* 14:219.